Supporting Information

Stacy et al. 10.1073/pnas.1400586111

SI Materials and Methods

Strains and Media. *Aggregatibacter actinomycetemcomitans* (*Aa*) and *Streptococcus gordonii* were cultured in filter-sterilized tryptic soy broth + 0.5% (wt/vol) yeast extract (TSBYE) medium. *Escherichia coli* was cultured in LB medium. Cultures were grown at 37 °C with shaking at 250 rpm oxically in a 5% CO_2 atmosphere, microoxically in a chamber (Coy) with a 5% O_2, 10% CO_2, and 85% N_2 atmosphere, or anoxically in a chamber (Coy) with a 5% H_2, 10% CO_2, and 85% N_2 atmosphere. Where appropriate, antibiotics were used at previously described selection and maintenance concentrations (1). Agar plates containing bovine liver catalase (Sigma-Aldrich) were made by equilibrating concentrated agar media to 42 °C and adding lyophilized catalase (suspended in 50 mM potassium phosphate buffer, pH 7.0) to give a final catalase activity concentration of 10,000 U mL^{-1}. *Aa* biofilms for monoculture experiments were formed by spotting 100 μL dense cell suspensions (OD = 0.5) onto 0.2-μm-pore–size polycarbonate filters (Whatman) placed onto the surface of tryptic soy agar + yeast extract (TSAYE) plates. Colony biofilms were moved to a fresh location on the plate after 24 h and further incubated anoxically for a total of 48 h before conducting experiments.

Strain Construction. The promoter fragment for generating a gene encoding the enzyme Dispersin B (*dspB*) transcriptional reporter construct (pYGK-pepB-β) was amplified from *Aa* 624 genomic DNA, digested, and ligated into pYGK-βGal (primers and restriction enzymes are listed in Table S4). The construct was electroporated into *Aa* 624 as previously described (2). Constructs for deleting the gene encoding the enzyme Dispersin B and *oxyR* from *Aa* 624 by natural transformation and homologous recombination were generated by using overlap extension PCR to fuse the 5′- and 3′-flanking regions of the target gene to an Spc^R cassette (*aad9*). One hundred nanograms each fragment was mixed and amplified using the following conditions: (*i*) 5 min at 94 °C; (*ii*) 3 cycles of 45 s at 94 °C, 45 s at 40 °C, and 3 min at 68 °C; (*iii*) 10 cycles of 45 s at 94 °C, 45 s at 45 °C, and 3 min at 68 °C; (*iv*) 15 cycles of 45 s at 94 °C, 45 s at 50 °C, and 3 min at 68 °C; (*v*) 10 cycles of 45 s at 94 °C, 45 s at 55 °C, and 3 min at 68 °C; and (*vi*) 10 min at 68 °C. Natural transformation of 624 was performed as previously described (3). Briefly, a 5- to 10-mL culture of 624 was pelleted, declumped by pestling, and spotted onto TSAYE + 5% heat-inactivated horse serum (Life Technologies). Spots were incubated for 24 h, collected, and resuspended in TSBYE. cAMP (Sigma-Aldrich) was added to a final concentration of 2 mM, and the suspension was respotted onto a fresh TSAYE + serum plate and incubated anoxically for 2 h to increase intracellular cAMP concentrations (4). The spot was then overlaid with 1 μg appropriate gene deletion construct and further incubated for 24 h before being resuspended and plated onto TSAYE with spectinomycin. Transformants were confirmed by PCR for replacement of the target gene with *aad9*. The *lysT* (5) promoter fragment for generating the constitutive mCherry construct (pPJ002) was amplified from *Aa* Y4 genomic DNA and fused by overlap extension PCR to mCherry amplified from pmCherry (Clontech). The fusion was digested and ligated into pJAK16 (primers and restriction enzymes are listed in Table S4). The construct was electroporated into *Aa* 624 as previously described (2).

β-Gal Assays. Biofilms were transferred to test tubes with rich media [tryptic soy broth + yeast extract (TSBYE)] and vortexed to remove attached cells. β-Gal activity was quantified using a luminescence assay (Galacto-Light Plus; Life Technologies) and microplate luminometer (Luminoskan Ascent; ThermoFisher Scientific). Raw luminescence values were normalized by total protein concentration determined using a standard Bradford assay on cells washed and boiled in 6 M urea.

Test Tube Dispersal Assay. *Aa* 624 was inoculated to an OD of 0.01 into test tubes with 2 mL rich media (TSBYE) and incubated anoxically with shaking for 24 h to form ring biofilms. Biofilms were gently washed, replaced with 4 mL media, and further incubated, either anoxically or oxically, with shaking for 48 h before being stained with crystal violet for visualization.

Microscopy. Abscess samples were resected from mice at the specified time point and immediately placed in coverwell imaging chambers (Electron Microscopy Sciences). For each chamber, ∼50–100 μL Prolong Gold antifade reagent (Invitrogen) was placed on the sample, sealed with a 45 × 50-mm coverglass (12–544-F; Fisherbrand), and then analyzed by confocal laser-scanning microscopy. All samples were visualized using an A1 confocal (Nikon) on a Ti-E inverted microscope (Nikon) equipped with a Plan Apo 10×/0.45 N.A. differential interference contrast (DIC) N1 objective (Nikon). Images were acquired using an N-STORM super resolution camera (Nikon) controlled with NIS-Elements Ar 4.13 software (Nikon). For each sample, multiple *Z* stacks were taken from distinct areas within the abscess, and optical sections within each *Z* stack were collected using a step size of 4.0–10.0 μm. All instrument settings were uniformly consistent and maintained between each set of experimental conditions. *Z*-stack images were then adjusted for γ, brightness, and contrast (identically for compared image sets) using NIS-Elements Ar 4.0 software (Nikon) before spatial distribution analysis. Images were generated in the Image Analysis Core Facility supported by Texas Tech University Health Sciences Center.

Operon Analysis. RNA from *Aa* VT1169 and 624 oxic liquid cultures was isolated for RT-PCR. cDNA synthesis with N_6 random primers and PCR on genomic DNA, cDNA, and RNA templates was performed as previously described (6) using primers targeting cotranscribed coding regions (Table S4).

RNA-seq. RNA isolation, next-generation sequencing library preparation, and computational methods were conducted as previously described (7).

1. Brown SA, Whiteley M (2007) A novel exclusion mechanism for carbon resource partitioning in *Aggregatibacter actinomycetemcomitans*. *J Bacteriol* 189(17):6407–6414.
2. Sreenivasan PK, LeBlanc DJ, Lee LN, Fives-Taylor P (1991) Transformation of *Actinobacillus actinomycetemcomitans* by electroporation, utilizing constructed shuttle plasmids. *Infect Immun* 59(12):4621–4627.
3. Wang Y, Goodman SD, Redfield RJ, Chen C (2002) Natural transformation and DNA uptake signal sequences in *Actinobacillus actinomycetemcomitans*. *J Bacteriol* 184(13):3442–3449.
4. Gwinn ML, Yi D, Smith HO, Tomb JF (1996) Role of the two-component signal transduction and the phosphoenolpyruvate: Carbohydrate phosphotransferase systems in competence development of *Haemophilus influenzae* Rd. *J Bacteriol* 178(21):6366–6368.
5. Jorth P, Whiteley M (2010) Characterization of a novel riboswitch-regulated lysine transporter in *Aggregatibacter actinomycetemcomitans*. *J Bacteriol* 192(23):6240–6250.
6. Korgaonkar AK, Whiteley M (2011) *Pseudomonas aeruginosa* enhances production of an antimicrobial in response to N-acetylglucosamine and peptidoglycan. *J Bacteriol* 193(4):909–917.
7. Jorth P, Trivedi U, Rumbaugh K, Whiteley M (2013) Probing bacterial metabolism during infection using high-resolution transcriptomics. *J Bacteriol* 195(22):4991–4998.

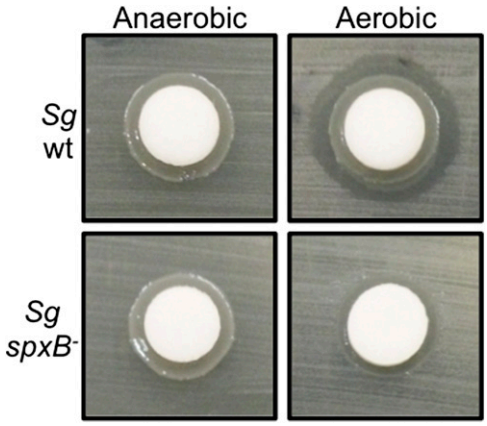

Fig. S1. Growth of *Aa* is inhibited by *S. gordonii* (*Sg*) in an H_2O_2-dependent manner. An overnight anoxic culture of *Aa* 624 was struck out as lawns onto rich media. Paper discs were placed onto the lawns and inoculated with 10^7 cfu exponential-phase *Sg* WT or *spxB*$^-$, a mutant that does not produce H_2O_2. Images were acquired after coculturing the bacteria overnight under anoxic or oxic growth conditions. Images are of one representative experiment.

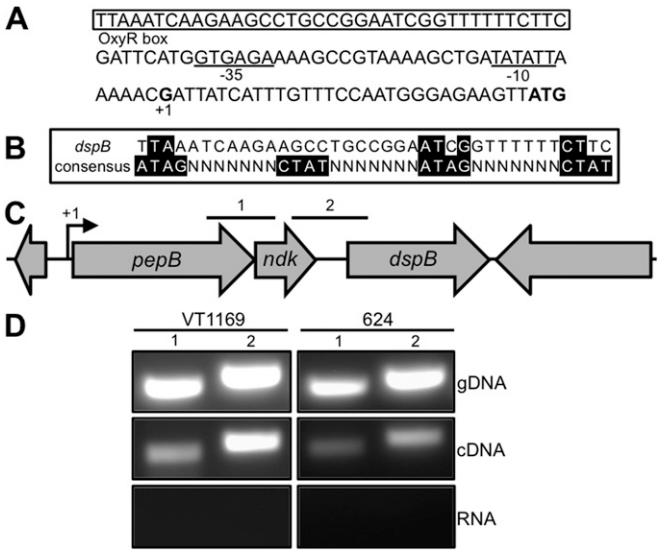

Fig. S2. The *dspB* promoter region and operon. (*A*) DNA sequence of the *dspB* promoter region. The start codon is in bold, the transcriptional start site is denoted by +1, putative σ^{70} promoter elements are underlined, and a putative OxyR operator is boxed. (*B*) Alignment to the consensus sequence shows that *dspB* has a degenerate OxyR binding sequence. (*C*) Structure of the *dspB* operon. Regions 1 and 2 correspond to the fragments amplified for the cotranscription analysis in *D*. (*D*) RT-PCR was used to show that *dspB* is in an operon with *pepB* and *ndk*. RNA for cDNA synthesis was extracted from oxic cultures of *Aa* strains VT1169 and 624. gDNA, genomic DNA.

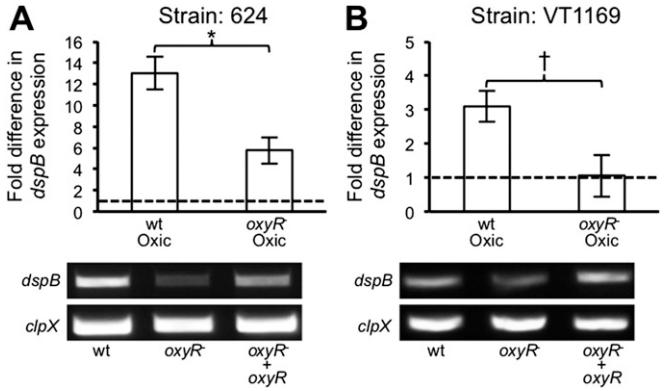

Fig. S3. *dspB* is regulated by OxyR. (*A*) β-Gal activity was quantified for anoxically grown *Aa* strain 624 WT or *oxyR*⁻ colony biofilms that were transferred to media alone or media supplemented with exogenous catalase (10,000 U mL^{-1}) and incubated under anoxic or oxic conditions for 6 h. (*Upper*) Fold difference in *dspB* expression (*y* axis) was determined by dividing the oxic expression value for each strain by its corresponding anoxic value. The dashed line represents anoxic expression (normalized to one within each replicate). Error bars represent SEM ($n = 3$). *$P < 0.025$ by a two-tailed Student *t* test. (*Lower*) Semi-quantitative RT-PCR was used to measure oxic *dspB* expression in WT, *oxyR*⁻, and complemented *oxyR*⁻ (*oxyR*⁻ + *oxyR*) strains. RNA for cDNA synthesis was harvested from anoxic biofilms that were transferred to oxic conditions for 6 h. The constitutively expressed *clpX* gene served as a loading control. (*B*) Same as *A* except with *Aa* strain VT1169. †$P < 0.06$ by a two-tailed Student *t* test.

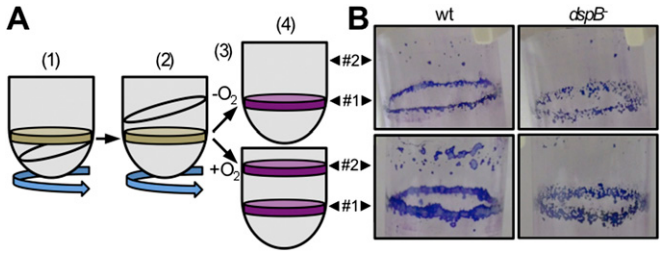

Fig. S4. *dspB* mediates dispersal in response to oxygen. (*A*) Qualitative test tube assay for monitoring biofilm dispersal. (1) *Aa* is initially grown as an anoxic shaking culture to form a ring biofilm (brown), (2) the media is replaced with a larger volume, (3) the culture is further incubated under anoxic ($-O_2$) or oxic ($+O_2$) conditions, and (4) detachment is assessed after crystal violet staining (purple). Biofilm dispersal is indicated by the development of a second ring biofilm (#2) located above the initial biofilm (#1). (*B*) Representative result of the test tube assay.

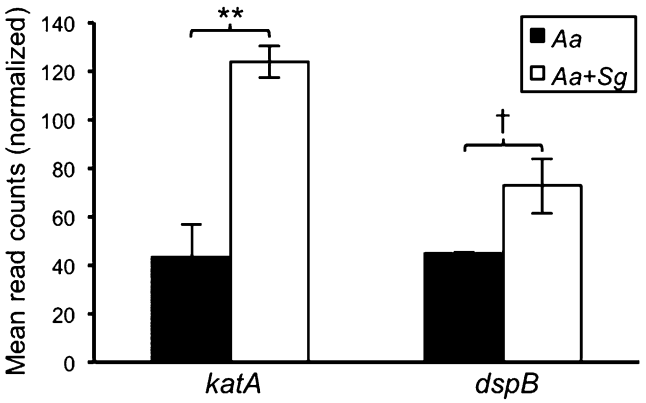

Fig. S5. The catalase gene (*katA*) and *dspB* transcription are enhanced during coculture in vivo with *Sg*. RNA-seq was used to measure *katA* and *dspB* gene expression within mono- and coinfected abscesses. Data analysis was performed as previously described (*SI Materials and Methods*). *Aa*, monoinfection; *Aa* + *Sg*, coinfection. Errors bars represent SEM. **$P < 0.0065$; †$P < 0.075$ by a two-tailed Student *t* test ($n = 3$).

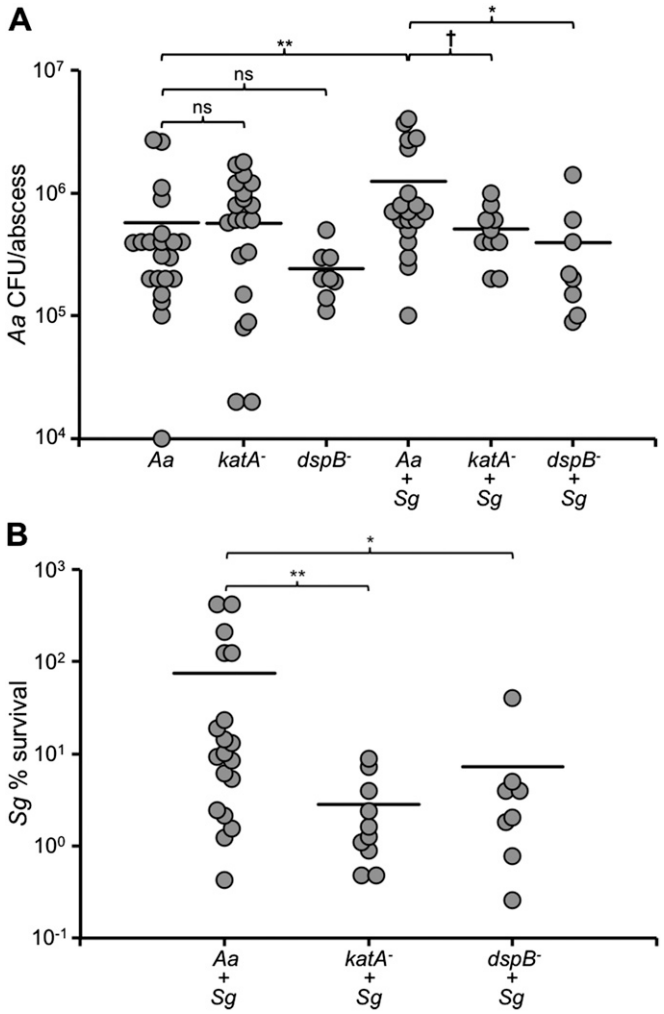

Fig. S6. *dspB* and *katA* enhance community-wide fitness in vivo. (*A*) *dspB* and *katA* are required for *Aa* polymicrobial synergy with *Sg*. Murine abscesses were formed using *Aa* WT (*Aa*), *katA*$^{-}$, *dspB*$^{-}$, and *Sg*. At 3 d postinfection, abscesses were harvested for enumerating viable bacteria on selective media. Each data point represents a single animal, and at least two biological replicates were performed for each condition. Horizontal bars represent the mean. Five *katA*$^{-}$ data points with values less than 10^4 cfu/abscess are not shown for visualization purposes. ns, not significant by a two-tailed Mann–Whitney U test. *$P < 0.015$; **$P < 0.005$; $^{\dagger}P < 0.075$ by a two-tailed Mann–Whitney U test. (*B*) *Sg* is less fit during coinfection with *Aa katA*$^{-}$ and *dspB*$^{-}$. Coinfected murine abscesses were harvested at 3 d postinfection to enumerate viable bacteria on selective media. Each data point represents a single animal, and at least two biological replicates were performed for each condition. Horizontal bars represent the mean. *$P < 0.04$; **$P < 0.005$ by a two-tailed Mann–Whitney U test.

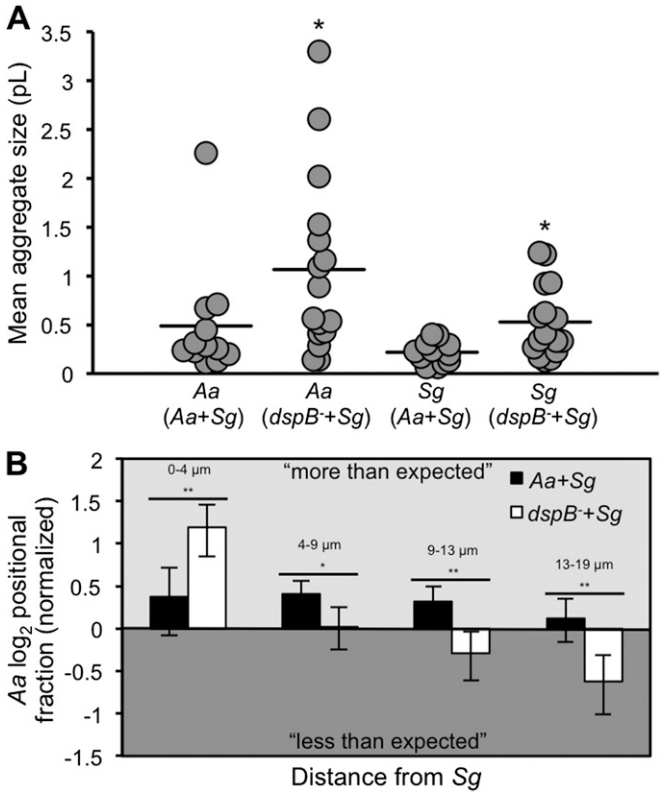

Fig. S7. DspB modulates community spatial structure in vivo. (*A*) Bacterial aggregates in vivo are larger when *Aa* cannot disperse. Each data point represents the mean aggregate size of either *Aa* or *Sg* within a single confocal *Z* stack [*Aa* + *Sg* ($n = 12$); *dspB*$^-$ + *Sg* ($n = 16$)]. For each species, aggregate sizes in *dspB*$^-$ + *Sg* infections were compared with aggregate sizes in *Aa* + *Sg* infections to determine statistical significance. *$P < 0.03$ by a two-tailed Mann–Whitney U test. (*B*) *Aa* that cannot disperse is located closer to *Sg*. *Aa* positional fraction is plotted as a histogram. Positional fraction here is defined as the proportion of total *Aa* biomass that is contained within defined micrometer ranges away from *Sg* aggregates. Positional fractions have been normalized, such that fractions above one ($\log_2 = 0$) occur more than expected, whereas fractions below one ($\log_2 = 0$) occur less than expected. Each column represents the mean, and the tested distances from *Sg* are indicated. The light gray region indicates positional fractions that were more than expected, and the dark gray region indicates positional fractions that were less than expected. Error bars represent 95% confidence intervals. *Aa* + *Sg* ($n = 12$); *dspB*$^-$ + *Sg* ($n = 16$). *$P < 0.05$; **$P < 0.01$ by a two-tailed Student *t* test.

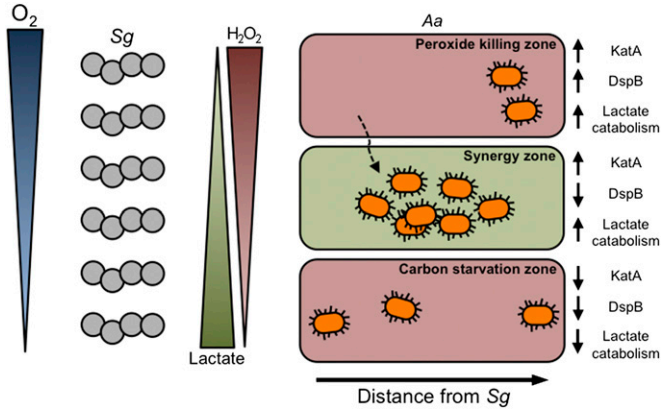

Fig. S8. Model for H_2O_2-supported L-lactate consumption by *Aa*. Oxygen levels control H_2O_2 and L-lactate production by *Sg*. In highly oxic regions, H_2O_2 is inhibitory to *Aa* and induces detoxification by KatA and dispersal by DspB. In less oxic regions, KatA converts H_2O_2 to oxygen and enables *Aa* L-lactate consumption. In anoxic regions, L-lactate is abundant but unavailable to *Aa* as a carbon source.

Table S1. *Aa* genes induced twofold or greater in the presence of oxygen

FC*	SD	ORF no.†	Description
2.00	1.33	AA0004	Conserved hypothetical protein
2.42	2.49	AA0019	Hypothetical protein
2.93	2.20	AA0024	DNA-binding protein, putative
2.59	1.88	AA0026	Hypothetical protein
4.68	4.63	AA0065	Hypothetical protein
3.36	1.24	AA0142	Glycerate kinase, putative
5.10	1.32	AA0143	Conserved hypothetical protein
3.86	1.18	AA0223	Catalase (*katA*)
2.38	1.53	AA0395	Conserved hypothetical protein
2.46	2.01	AA0396	Conserved hypothetical protein
3.54	1.07	AA0546	Cytochrome *c*-type protein, putative
3.03	1.06	AA0547	Diheme cytochrome C napB precursor, putative
3.73	1.06	AA0549	Ferredoxin-type protein, putative
4.00	1.08	AA0550	Ferredoxin-type protein, putative
4.36	1.13	AA0551	Hypothetical protein
3.67	1.04	AA0551	Hypothetical protein
3.36	1.09	AA0552	Periplasmic nitrate reductase precursor, putative
5.46	1.55	AA0553	NapD protein, putative
2.00	2.72	AA0631	Hypothetical protein
2.69	2.25	AA0633	Hypothetical protein
2.22	1.13	AA0708	Cysteine desulfurase, putative
2.22	1.09	AA0709	Conserved hypothetical protein
2.22	1.16	AA0715	Ferredoxin 2Fe-2S, putative
2.73	1.04	AA0716	Conserved hypothetical protein
2.98	1.33	AA0719	Hypothetical protein
2.83	1.30	AA0719	Hypothetical protein
3.42	1.32	AA0721	Conserved hypothetical protein (*dspB*)
3.25	1.19	AA0722	Nucleoside diphosphate kinase, putative
3.14	1.18	AA0723	Cytosol aminopeptidase, putative
3.31	1.30	AA0795	Iron compound ABC transporter, substrate-binding protein, putative
2.88	1.26	AA0796	Iron compound ABC transporter, permease protein, putative
2.83	1.19	AA0798	Iron compound ABC transporter, permease protein, putative
2.59	1.23	AA0799	Vibriobactin and enterobactin ABC transporter, ATP-binding protein, putative
2.11	4.33	AA0803	Hypothetical protein
2.11	1.37	AA1048	Major ferric iron-binding protein, putative
2.93	4.77	AA1212	Hypothetical protein
2.59	2.47	AA1395	Conserved hypothetical protein
2.07	2.24	AA1531	Hypothetical protein
2.51	1.36	AA1604	Conserved hypothetical protein
2.38	2.86	AA1620	Hypothetical protein
2.34	1.59	AA1640	Conserved hypothetical protein
2.59	1.80	AA1823	Hypothetical protein
2.73	1.38	AA1824	Not yet annotated
2.55	1.28	AA1825	Iron(III) ABC transporter, permease protein, putative
2.78	1.30	AA1826	Iron(III) ABC transporter, putative
2.88	1.47	AA1827	Iron(III) ABC transporter, periplasmic-binding protein, putative
2.98	1.46	AA1840	Conserved hypothetical protein
2.42	2.50	AA1904	Hypothetical protein
2.00	2.15	AA1908	Conserved hypothetical protein
2.98	2.03	AA1911	Hypothetical protein
3.03	1.06	AA1984	Tellurite resistance protein, putative
2.88	1.54	AA2034	Ferredoxin-NADP reductase, putative
2.42	2.92	AA2074	Hypothetical protein
2.42	1.27	AA2123	Hypothetical protein
2.14	1.46	AA2436	Conserved hypothetical protein
5.37	1.50	AA2485	Adhesin invasin, putative (*apiA*)
2.69	1.31	AA2495	Conserved hypothetical protein
2.88	1.20	AA2521	Conserved hypothetical protein
2.83	1.21	AA2532	Conserved hypothetical protein
2.30	4.51	AA2546	Hypothetical protein

Table S1. Cont.

FC*	SD	ORF no.†	Description
4.44	2.06	AA2593	Conserved hypothetical protein
2.11	5.96	AA2798	Hypothetical protein
3.54	1.95	AA2865	Not yet annotated
2.00	1.84	AA2921	Conserved hypothetical protein
2.18	4.12	AA3016	Hypothetical protein

*Fold changes (FCs) are relative to anoxic gene expression and represent the average of four pairwise comparisons.
†ORF numbers are from the *Aa* HK1651 genome annotations (www.genome.ou.edu/act.html).

Table S2. *Aa* genes induced twofold or greater in the absence of oxygen

FC*	SD	ORF no.†	Description
4.52	2.47	AA0025	Hypothetical protein
4.92	1.77	AA0031	Hypothetical protein
2.46	1.26	AA0041	Formate-dependent nitrite reductase, putative
6.50	1.20	AA0043	Polysulfide reductase, putative
5.56	1.14	AA0044	Nitrite reductase, iron-sulfur protein, putative
7.73	1.09	AA0046	Nitrite reductase, cytochrome *c*-type protein, putative
8.72	1.30	AA0047	Cytochrome *c* nitrite reductase, catalytic subunit NrfA, putative
3.73	1.13	AA0069	Conserved hypothetical protein
2.64	1.33	AA0236	Anaerobic ribonucleoside-triphosphate reductase, putative
2.59	1.35	AA0288	Conserved hypothetical protein
2.14	1.46	AA0290	Conserved hypothetical protein
2.00	1.41	AA0478	Phosphotransferase system, mannose-specific IIAB component, putative
2.00	1.44	AA0495	Hypothetical protein
5.01	1.23	AA0804	Fumarate reductase flavoprotein subunit, putative
4.59	1.20	AA0805	Fumarate reductase iron-sulfur protein, putative
5.66	1.06	AA0806	Fumarate reductase 15 kDa hydrophobic protein, putative
6.84	1.17	AA0807	Fumarate reductase 13 kDa hydrophobic protein, putative
2.78	2.80	AA0852	Hypothetical protein
3.67	1.36	AA0853	Hypothetical protein
2.59	1.26	AA0854	ABC transporter, permease protein, putative
2.26	1.22	AA0855	ABC transporter, permease protein, putative
2.14	1.26	AA0856	ABC transporter, periplasmic arginine-binding protein precursor, putative
2.26	1.33	AA0858	ABC transporter, ATP-binding protein, putative
3.61	1.31	AA1137	Anaerobic dimethyl sulfoxide reductase chain a, putative
3.61	1.41	AA1138	Anaerobic dimethyl sulfoxide reductase chain B, putative
3.14	1.36	AA1140	Anaerobic dimethyl sulfoxide reductase chain c, putative
2.46	1.39	AA1141	Conserved hypothetical protein
2.00	1.35	AA1318	Hypothetical protein
2.46	1.82	AA1379	Glycerophosphoryl diester phosphodiesterase, putative
2.42	1.49	AA1383	DprA protein, putative
2.34	1.68	AA1692	Hexulose-6-phosphate synthase, putative
2.93	1.74	AA1694	Not yet annotated
2.51	1.79	AA1695	Conserved hypothetical protein
2.30	1.12	AA1717	Fumarate hydratase class II, putative
2.22	1.24	AA1758	Hydrogenase isoenzymes nickel incorporation protein hypB, putative
2.51	1.04	AA1759	Not yet annotated
2.73	1.23	AA1760	Hydrogenase expression formation protein, putative
2.07	1.13	AA1767	Hypothetical protein
2.00	1.10	AA1769	Hypothetical protein
5.10	1.60	AA1839	Bacteriophage transcriptional regulator, putative
2.78	2.93	AA1950	Spermidine putrescine ABC transporter, permease protein, putative
3.73	1.69	AA2028	Conserved hypothetical protein
3.54	2.30	AA2149	Conserved hypothetical protein
2.34	1.72	AA2190	Hydrogenase assembly chaperone HypC, putative
5.46	1.28	AA2193	Oxaloacetate decarboxylase γ-subunit, putative
5.37	1.41	AA2195	Oxaloacetate decarboxylase α-subunit, putative
5.56	1.72	AA2196	Oxaloacetate decarboxylase β-subunit, putative
3.61	2.53	AA2199	Hypothetical protein
2.42	1.17	AA2231	Dethiobiotin synthetase, putative
15.45	1.22	AA2250	Cytochrome *c*-type protein, putative
12.13	1.06	AA2251	Biotin sulfoxide reductase, putative
2.73	1.45	AA2540	5-Methyltetrahydropteroyltriglutamate-homocysteine methyltransferase, putative
2.30	1.33	AA2565	Transketolase, N-terminal subunit, putative
2.11	1.30	AA2566	Conserved hypothetical protein
2.18	1.42	AA2567	Hypothetical protein
3.19	1.43	AA2595	Cytochrome c551 peroxidase, putative
2.38	1.39	AA2682	Not yet annotated
9.35	1.23	AA2683	Conserved hypothetical protein
5.56	1.53	AA2684	Conserved hypothetical protein
4.52	1.46	AA2686	Hypothetical protein
13.00	3.19	AA2687	Na^+ H^+ antiporter component, putative
6.96	1.16	AA2688	Not yet annotated

Table S2. Cont.

FC*	SD	ORF no.†	Description
7.09	1.45	AA2689	Hypothetical protein
7.34	1.25	AA2691	Hypothetical protein
5.66	1.26	AA2692	Hydrogenase, putative
6.06	1.29	AA2693	Not yet annotated
5.01	1.38	AA2695	Not yet annotated
4.07	1.46	AA2696	Not yet annotated
3.19	1.37	AA2697	Not yet annotated
5.96	1.31	AA2698	Formate dehydrogenase, α-subunit, putative
5.86	1.13	AA2699	Formate dehydrogenase, α-subunit
2.59	2.58	AA2705	Hypothetical protein
2.42	1.26	AA2706	2-Oxoglutarate dehydrogenase, E1 component, putative
5.96	1.13	AA2716	Not yet annotated
2.07	1.26	AA2726	Not yet annotated
8.57	1.38	AA2784	Not yet annotated
2.51	1.26	AA2805	Leukotoxin secretion ATP-binding protein
2.11	1.35	AA2807	Leukotoxin-activating lysine-acyltransferase
2.51	1.67	AA2808	Hypothetical protein
2.69	1.61	AA2876	Hypothetical protein
3.67	1.70	AA2969	β-Eliminating lyase, putative
2.59	1.73	AA2970	β-Eliminating lyase, putative
2.69	2.40	AA2972	β-Eliminating lyase, putative

*Fold changes (FCs) are relative to anoxic gene expression and represent the average of four pairwise comparisons.
†ORF numbers are from the *Aa* HK1651 genome annotations (www.genome.ou.edu/act.html).

Table S3. Strains and plasmids used in this study

Strain or plasmid	Description	Source
Aa		
VT1169	WT, Nal^R Rif^R	1
VT1169 *oxyR*$^-$	*oxyR* null mutant, Spc^R	2
624	WT	3
624 *oxyR*$^-$	*oxyR* deletion mutant, Spc^R	This study
624 *dspB*$^-$	*dspB* deletion mutant, Spc^R	This study
E. coli		
DH5α	endA1 hsdR17 supE44 thi-1 recA1 Δ(lacZYA-argF) U169, deoR [Φ80dlac Δ(lacZ)M15]	4
Sg		
Challis DL1.1	WT	ATCC 49818
Challis *spxB*$^-$	*spxB* null mutant, Spc^R	5
Challis GFP	Constitutive GFP	This study
Plasmids		
pYGK-βGal	pYGK expression vector with promoterless *lacZ*, Kan^R	6
pYGK-pepB-β	pYGK-βGal with *pepB* promoter region, Kan^R	This study
pYGS-OxyRC	*oxyR* complementation vector	2
pGEM-T Easy	TA cloning vector, Amp^R	Promega
pVT1461	Source of *aad9*	7
pmCherry	Source of mCherry	Clontech
pJAK16	Expression vector	8
pPJ002	*lysT* promoter-mCherry fusion	This study

1. Mintz KP (2004) Identification of an extracellular matrix protein adhesin, EmaA, which mediates the adhesion of *Actinobacillus actinomycetemcomitans* to collagen. *Microbiol* 150(8): 2677–2688.
2. Ramsey MM, Whiteley M (2009) Polymicrobial interactions stimulate resistance to host innate immunity through metabolite perception. *Proc Natl Acad Sci USA* 106(5):1578–1583.
3. Jorth P, Whiteley M (2012) An evolutionary link between natural transformation and CRISPR adaptive immunity. *mBio* 3(5):e00309–12.
4. Sambrook JFE, Maniatis T (1989) *Molecular Cloning: A Laboratory Manual* (Cold Spring Harbor Lab Press, Plainview, NY).
5. Kreth J, Zhang Y, Herzberg MC (2008) Streptococcal antagonism in oral biofilms: *Streptococcus sanguinis* and *Streptococcus gordonii* interference with *Streptococcus mutans*. *J Bacteriol* 190(13):4632–4640.
6. Brogan JM, Lally ET, Demuth DR (1996) Construction of pYGK, an *Actinobacillus actinomycetemcomitans-Escherichia coli* shuttle vector. *Gene* 169(1):141–142.
7. Mintz KP, Brissette C, Fives-Taylor PM (2002) A recombinase A-deficient strain of *Actinobacillus actinomycetemcomitans* constructed by insertional mutagenesis using a mobilizable plasmid. *FEMS Microbiol Lett* 206(1):87–92.
8. Kachlany SC, et al. (2000) Nonspecific adherence by *Actinobacillus actinomycetemcomitans* requires genes widespread in bacteria and archaea. *J Bacteriol* 182(21):6169–6176.

Table S4. Primers used in this study

Function/name	Sequence (5′ → 3′)	Underlined region*
Operon RT-PCR		
Region 1		
Operon-1-F	ACTGCCACCGCTTTTTTATCC	
Operon-1-R	TTTGGCAGCGTTCTCAGGGTTAG	
Region 2		
Operon-2-F	CACGATTCGCCGTGATTTTGC	
Operon-2-R	CCGCACGTTGATTAAGTAAATGGC	
dspB transcriptional reporter		
pepB promoter		
pepB-pro-F	GGGGTACCCCACTGCCTTTATTGATGCGCAG	KpnI
pepB-pro-R	CGGGATCCCGAACTTCTCCCATTGGAAACAAATG	BamHI
oxyR deletion construct		
5′-Flanking region		
oxyR-UP-F	AAGTGCGGTACGCTTCTAAATCATCACTGC	USS
oxyR-UP-R	CATGTATTCACGAACGAAAATCGAGATCCTCAATTATAGAAGGTAGC	Overlaps with *aad9*
3′-Flanking region		
oxyR-DN-F	GAAAACAATAAACCCTTGCATATGTGGGGTAAGCTATGGTCG	Overlaps with *aad9*
oxyR-DN-R	AAGTGCGGTCCGAAATGGGGAACAACC	USS
dspB deletion construct		
5′-Flanking region		
dspB-UP-F	AAGTGCGGTATGGATGATAACTTGGTCGGC	USS
dspB-UP-R	CATGTATTCACGAACGAAAATCGTGTCCAGCATTAATCCGGTCT	Overlaps with *aad9*
3′-Flanking region		
dspB-DN-F	GAAAACAATAAACCCTTGCATATGAAATAGATTGCTAACGCGTGTTCA	Overlaps with *aad9*
dspB-DN-R	AAGTGCGGTACGGCAATGTGATTCAAGGTT	USS
Spc^R cassette (*aad9*)		
SpcR-F	CGATTTTCGTTCGTGAATACATG	
SpcR-R	CATATGCAAGGGTTTATTGTTTTC	
Constitutive mCherry		
lysT promoter		
lysT-pro-F	TGACGGATCCACTTGTGTAGAGGTGCAAAC	BamHI
lysT-pro-R	CCTCCTCGCCCTTGCTCACCATTTGTTCTTCCTAATATTAAGGGAGAAC	
mCherry		
cherry-F	CCCTTAATATTAGGAAGAACAAATGGTGAGCAAGGGCG	
cherry-R	TGACAAGCTTCGCTACTTGTACAGCTCGT	HindIII
Semiquantitative RT-PCR		
dspB		
dspB-F	TATTTTATCTCTTTTCCTACTGGG	
dspB-R	CACTCATCCCCATTCGTC	
clpX		
clpX-F	GCAGAAACCATGGCGCGTATG	
clpX-R	CAATTCGCTTAATGGCGCCAC	

*Represents the restriction site, overlap extension sequence, or uptake signal sequence (USS).

Other Supporting Information Files

Dataset S1 (XLS)